

Experimental tests of LiSn alloys as potential liquid metal for the divertor target in a fusion reactor



F.L. Tabarés*, E. Oyarzabal, A.B. Martín-Rojo, D. Tafalla, A. de Castro, F. Medina, M.A. Ochando, B. Zurro, K. McCarthy, the TJ-II Team

Fusion National Laboratory CIEMAT, Av Complutense 40, Madrid 28040, Spain

ARTICLE INFO

Article history:

Received 11 July 2016

Revised 21 October 2016

Accepted 26 November 2016

Available online 26 December 2016

Keywords:

Plasma facing Materials

Liquid metals

LiSn alloys

Hydrogen retention

Reactor materials

ABSTRACT

The first experiments of exposure of a LiSn alloy (Li/Sn atomic ratio = 20/80) to a hydrogen plasma in TJ-II are here presented. Solid and liquid samples have been inserted at the edge and evidence of sample melting of a solid sample during plasma exposure has been observed. A negligible perturbation of the plasma has been recorded, even when stellarator plasmas are particularly sensitive to high Z elements due to the tendency to central impurity accumulation. Melting of the sample by the plasma thermal load did not lead to any deleterious effect on the plasma performance. Strong lithium emission was detected at the LiSn sample but no sign of Sn contamination and low values of Z_{eff} and radiated power were deduced. Hydrogen recycling was studied at two different temperatures and no change was detected in the range of 300–750 K. The retention of H₂ by the alloy was addressed in separate experiments at the laboratory. Values in the order of 0.01% H/(Sn + Li) were deduced in agreement with in situ TDS analysis of the plasma exposed samples and previous reports.

© 2016 Elsevier Ltd.

This is an open access article under the CC BY-NC-ND license.

(<http://creativecommons.org/licenses/by-nc-nd/4.0/>)

1. Introduction

Among the possible liquid metals (LM) presently considered as candidates for the development of an alternative solution to the Power Exhaust Handling in a future Fusion Reactor (Li, Sn, Ga), tin lithium alloys offer unique properties in terms of evaporation, fuel retention and plasma compatibility. This is the reason why this particular LM was chosen as main candidate in the US APEX project [1]. Although the sputtering and evaporation characteristics were tested at the laboratory level, confirming the preferential sputtering and evaporation of the Li component in the molten phase, no hot plasma testing was ever performed. For the same temperature, similar values of Li sputtering yield by D ions was found for liquid Li and liquid LiSn alloys, with a basically identical ion composition of the sputtered Li [2]. However, evaporation rates from the alloy are up to a factor of 1000 lower than from the pure Li metal. Very recently, a LiSn (30:70at.%) alloy has been exposed to ISTTOK tokamak and very promising results on D retention and surface segregation of Li were obtained [3]. Motivated by these results a full campaign of LiSn testing in TJ-II plasmas has been initiated. In addition to these hot plasma tests, laboratory ex-

periment aimed at evaluating the H retention characteristics and the secondary electron emission of LiSn surfaces at several temperatures were undertaken. Also, in situ desorption of D after exposure to TJ-II plasmas was carried out.

In this work, an account of the results obtained and their implications for the use of LiSn alloys as divertor material solution for a future Fusion Reactor is given.

2. Experimental set-up

2.1. Sample preparation

For the experiments reported here, a commercially available LiSn alloy (Princeton Sci. Corp., Easton, PA, USA) with a Li: Sn atomic ratio of 20:80 was used.

Due to the presence of several eutectics in the LiSn phase diagram [4], achieving a homogeneous liquid phase by direct melting of the LiSn sample may be challenging. Formation of slag on top of the molten phase is commonly observed, thus preventing the production of a clean, single liquid entity. It was found that strong stirring during the first time the alloy is melted down in an oven was mandatory in order to get a homogeneous liquid phase. Once this is achieved, cooling down to the solid phase again produces a smooth, clean surface and no further stirring is needed anymore.

* Corresponding author.

E-mail address: tabares@ciemat.es (F.L. Tabarés).

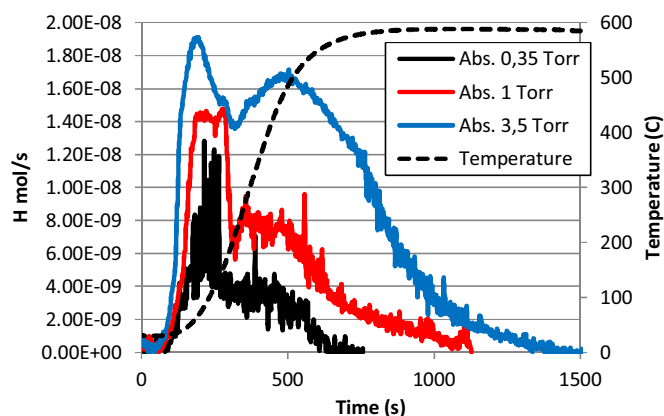


Fig. 1. TDS spectra of hydrogen desorption from a LiSn alloy (20:80) exposed to several pressures of H₂ at 425 °C. The peak at ~200 °C corresponds the decomposition of lithium hydroxide.

This procedure was essential when addressing the impregnation of a metallic mesh with the liquid alloy.

2.2. Set-ups

Two kinds of set-up were used depending on the experiment: a vacuum chamber for laboratory retention experiments and a manipulator system with a vacuum lock for exposures in TJ-II, as described in the following paragraphs.

For the absorption experiments (Fig. 1), the oven is charged with solid LiSn. Prior to the absorption experiments, the sample is heated up to 550 °C for conditioning purposes. Once the sample has been outgassed and cooled down, it is heated again up to the desired temperature and the valve to the pumping system is closed. After that, the chamber is filled to the required pressure of H₂ (0.35, 1 and 3.50 Torr respectively) by expansion from a pre-filled reservoir at pressures 100× higher than those required (35, 100 and 350 Torr respectively)

3. Results

3.1. Laboratory studies

In principle, the quantity of absorbed H after a given time can be simply evaluated from the resulting pressure drop in the sealed experimental chamber. However, due to the low values of hydrogen retention in LiSn the change in pressure during the absorption to monitor the absorbed quantity is not accurate enough in the present set up as to obtain any reliable absorption results. Therefore only the results regarding the Thermal Desorption Spectroscopy (TDS) measurements after exposure to H₂ at to different temperatures and pressures will be shown in this section. The absorption experiments are only carried out in order to reach the hydrogen equilibrium mole fraction in the LiSn for the different conditions. The absorption time is long enough as to achieve absorption equilibrium in the LiSn for each condition, this is confirmed by repeating the absorption in one condition for two different absorption times and corroborating that the desorbed quantity in the TDS is the same for both cases. We use absorption times of 1 h though we have observed that the equilibrium is already reached after 15 min in all conditions here tested.

Fig. 1 shows the results of the TDS for the case of absorption at 425 °C for three different absorption pressures (0.35, 1 and 3.5 Torr) for the calibrated pure hydrogen signal at amu = 2, and with the background subtracted. Because of the small values of absorption (therefore desorption) in LiSn the background signal

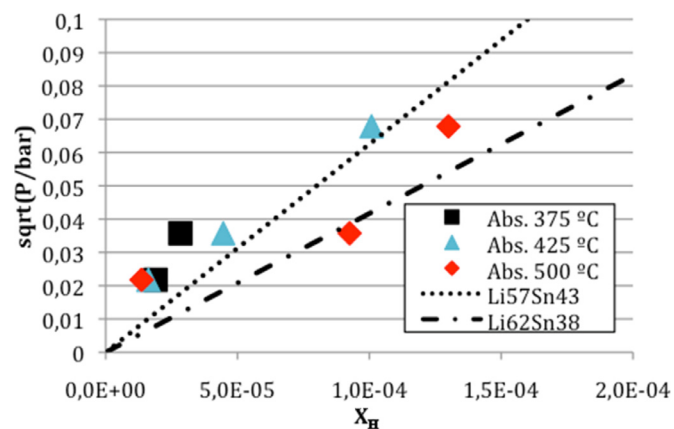


Fig. 2. Siebert's plot of the solubility of H in LiSn (20:80). Data from the present work at several temperatures are shown together with previous measurements at different Li: Sn ratios and the fitting there displayed (Ref. [5]).

due to the desorption over time of the chamber walls (which are slowly heated during the TDS) is not negligible with respect to the desorbed quantity and must be subtracted from the raw data of the Quadrupole Mass Spectrometer (QMS). As expected the desorbed quantity increases for increasing absorption pressure indicating that the solubility limit (i.e., onset of hydride formation) has not been reached in the studied pressure range at the studied temperature, if this was the case the desorbed amount after saturation should remain constant, and a peak at higher temperatures, corresponding to the HLi decomposition, should be observed. This behaviour was expected based on previous literature data [5], which shows hydride formation pressures over 7000 Torr for other mixtures of LiSn. The comparison with these results, shown in Fig. 2, is discussed in more detail later. The TDS for the three pressures presents desorption peaks at similar desorption temperatures, one or two (it is not clear) at low temperatures (probably related with hydroxide desorption) and a second peak at around 400–500 °C. This second peak agrees well with the desorption peak of pure lithium observed in previous experiments [6]. Even though only the results for absorption at 425 °C are shown for clarity the TDS for the two other studied temperatures presents desorption peaks at similar temperatures and the same evolution with the absorption pressure.

3.2. Plasma exposure in TJ-II

Several methods of exposing LiSn to the hot plasmas of TJ-II [7] were tested. Only ECR heated plasmas (600 kW, 53 GHz, 2nd harmonic) were used in these tests. The main limiter was a CPS Liquid Lithium system kept at T > 200 °C in all cases, and the first wall was covered by a lithium layer. The basic set up used for the insertion of LiSn samples into the plasma edge was the same as that previously used for lithium exposures [8]. Three different samples were used: a solid piece of LiSn, a mesh of Mo partially embedded in molten LiSn, a SS mesh fully embedded in molten LiSn and a direct deposition of the alloy on the SS bar made by dipping the “finger” into the molten alloy. The temperature of the “finger” was varied in the SS mesh case and a thermocouple attached to the base was used for its monitoring. In this way, the comparative behaviour of solid and liquid LiSn (melting temperature = 330 °C) could be addressed.

Fig. 3 shows the traces of the main plasma parameters for selected shots, summarized in Table 1. They include shots without bar insertion (#41562, at -4 cm) and with insertion at the LCFS but at two different initial temperatures of the LiSn alloy (#41569 at 120 °C and #41573 at 440 °C). For the examples shown here, to-

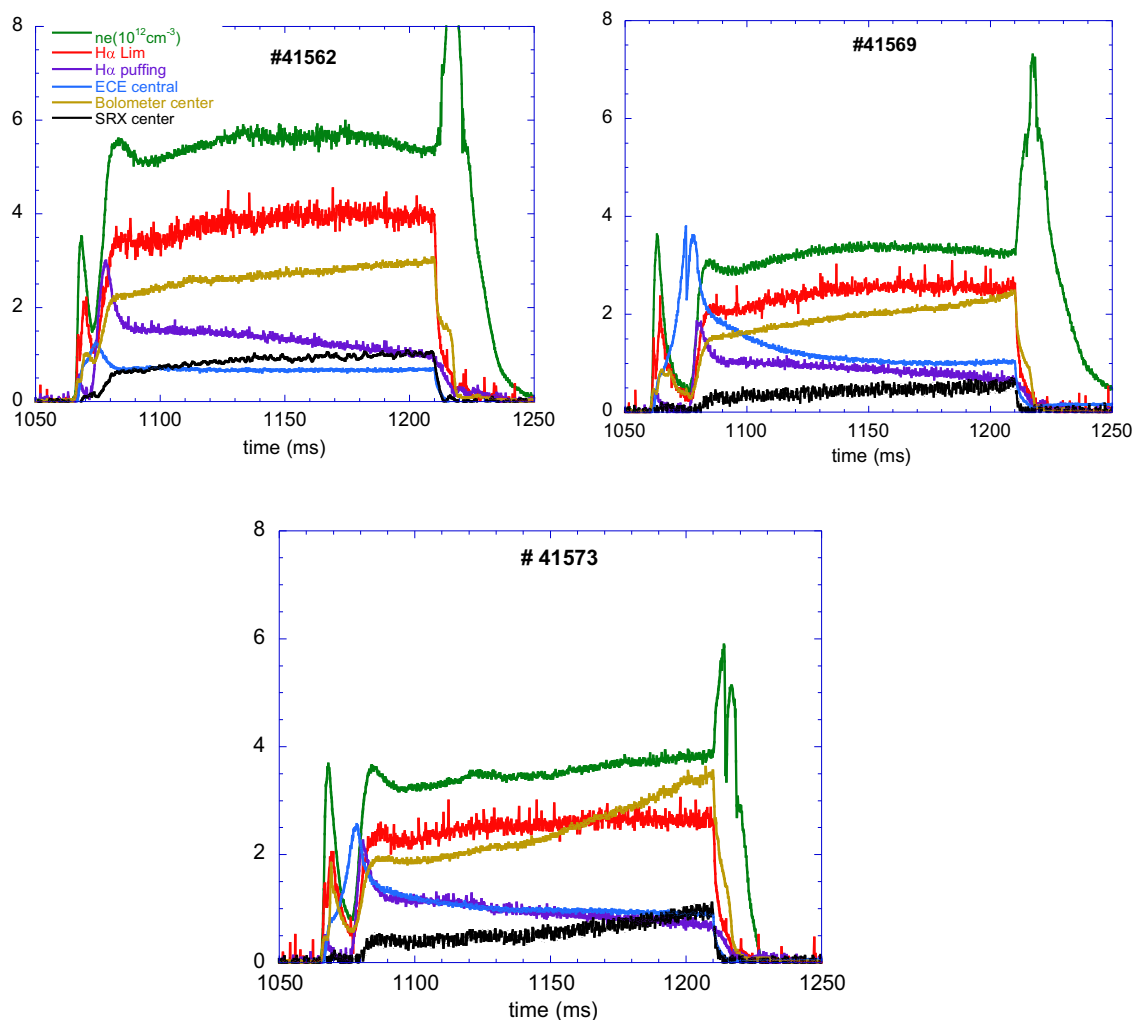


Fig. 3. Traces of the main plasma parameters for the reference shots used in this work and summarized in Table 1. Line average electron density, H_{α} at the main limiter, H_{α} corresponding to the gas fuelling, central ECE signal (Te), central integrated bolometer (total radiation) and Soft X ray signals are displayed.

Table 1
Summary of plasma conditions for reference shots.

Shot #	Finger location	LiSn T (°C)	Electron density (10^{13} cm^{-3})	Te (a) eV
41562	Out (−4 cm)	50	0.50	50
41569	LCFS	120	0.33	65
41573	LCFS	440	0.34	60

tal radiation values, as well as Soft X Ray emission, were very similar to those observed when a pure lithium sample was exposed to the plasma in TJ-II, with total radiation powers below 10 kW. Fig. 4 shows the value of the density normalized total radiation (from bolometry), and in Fig. 5, the reconstructed values of Z_{eff} are displayed. Values below 1.5 were generally obtained although a time increase of this parameter, up to 1.8, can be seen for the case of hot finger insertion. This behaviour can be ascribed to the progressive increase of the evaporated Li flow as the sample is heated by the plasma. A search for characteristic Sn I and Sn II lines in the visible, as well as Sn III and Sn IV lines in the VUV (50–80 nm), did not yield evidence of the presence of tin in the plasma even for the most potentially perturbing conditions.

Fig. 6 shows some representative traces of Li, Li^+ and H_{α} emissions. As seen, Li related signals show a fast increase with time while the H_{α} signal remains fairly constant. In order to get some

insight into the recycling properties of the alloy, the local H_{α} signal recorded in front of the finger is normalized to the H_{α} signal from the main CPS Li limiter, kept at constant temperature all through the experiment. The results for several initial temperatures and plasma flows are displayed in Fig. 7. While in shots #68 and 69 the LiSn sample was heated only by the plasma, in #72 and 73 it was intentionally heated externally at 440 °C before plasma exposure. However, there is no difference in the time evolution of the recycling characteristics, since the plasma fluxes are similar. For lower plasma densities (fluxes), a progressive increase of the local/global H_{α} signal takes place at 440 °C, finally reaching the same value as those at higher densities. This type of increase is not seen for the low density/low T sample, however.

When LiSn was directly applied to a bare SS bar, i.e., with no mesh structure in between, a systematic collapse of the plasma after a few tens of milliseconds was seen. Due to the characteristics of microwave absorption by the plasma, ECRH becomes inefficient at densities above the cut-off limit (line average density of $\sim 1 \times 10^{19} \text{ m}^{-3}$ in TJ-II). This limiting density was quickly achieved in the referred discharges; thus, precluding a possible analysis of a potential radiative collapse by massive impurity injection, as indicated by spectroscopic data. Although the reason of such behaviour is not understood, and no visual access to the sample was possible during the machine operation, one may speculate about a fast melting of the alloy by the plasma load followed by dripping into

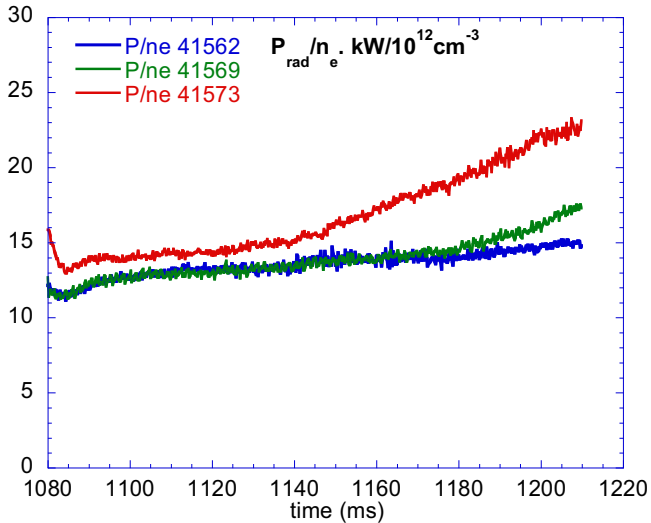


Fig. 4. Total radiation normalized to the average density for the three shots displayed in Table 1.

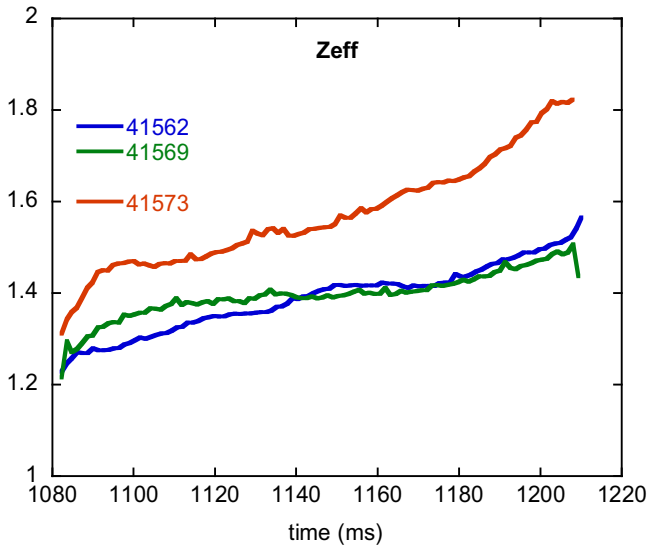


Fig. 5. Time evolution of Z_{eff} during the three reference shots deduced from soft X ray emission (SXR) traces.

the vacuum chamber or receding from the plasma-wetted area, thus eventually leaving a bare SS surface exposed to the plasma.

Finally, the full particle balance during the operation day was analysed. The total H_2 fuelled during the day was estimated from the calibrated puffing signal while the desorbed amount after each discharge was recorded by mass spectrometry and then integrated over the 50 shots produced. An average recycling coefficient of $R=0.1$ was deduced in this way, starting at lower values at the beginning of the day. The CPS finger was outgassed in a separate chamber without exposing it to the air. Even so, traces of water, CO/N_2 and CO_2 were recorded during the TDS, as seen in Fig. 8. While the total amount of missing H was estimated in 6×10^{21} atoms, integration of the mass 2 recovered during the TDS yielded only $6,2 \times 10^{19}$ H atoms. Due to the small amount of H recovered and the contribution of mass 2 by other molecules, mainly water, present at higher concentrations, the direct ratio between the desorbed hydrogen and that retained in all the plasma facing components, such as first wall and main limiter, of 1% must be considered only as a maximum value. For a mass of the interact-

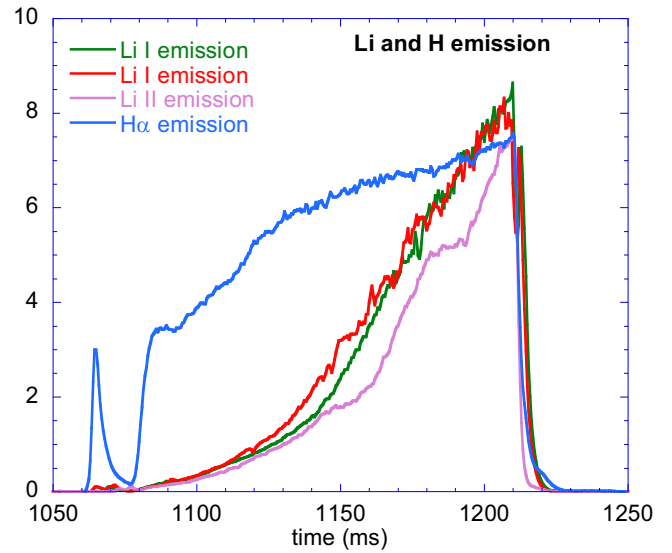


Fig. 6. Example of the time evolution of some characteristic emission lines during the plasma shot. LiI (671 nm), LiII (538 nm) and $H\alpha$ (656 nm). Two examples of Li emission corresponding to solid (cold) and liquid (hot) LiSn initial state are shown, although their absolute magnitudes cannot be compared as they correspond to different locations in the plasma periphery. The strong rise of the corresponding lithium signals indicates heating of the sample by the plasma. Note their negligible value at the beginning of the shot, indicating evaporation-dominated ejection of the Li atoms. A delay in the emission of Li from the cold finger of ~60–80 ms is apparent in the figure.

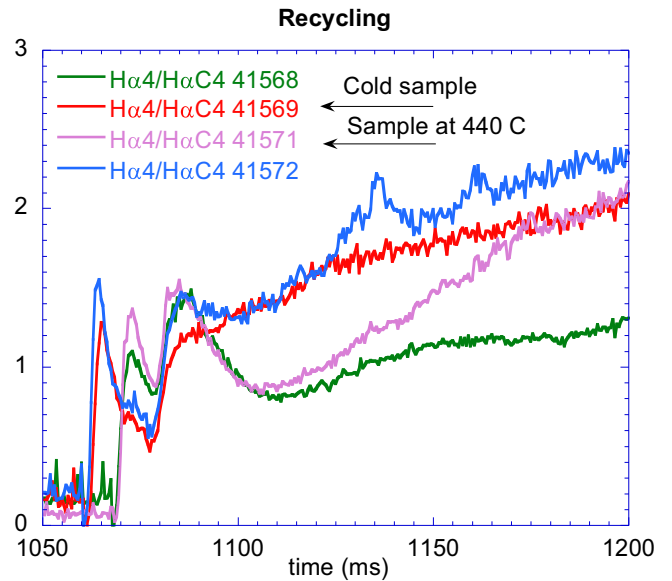


Fig. 7. Normalized local $H\alpha$ signals (from the LiSn finger) to the total plasma flux ($H\alpha$ from the main limiter) for two different initial temperatures and different plasma densities. Note the same recycling characteristics for the cold and hot cases at similar densities.

ing alloy area of 1 g, this retention implies H/(LiSn) atom ratios of <1%.

4. Discussion

4.1. Laboratory retention experiments

In order to obtain the equilibrium H mole fraction (X_H) at each studied condition from the TDS results, the integral of the calibrated P_{H_2} vs. time for each case is first evaluated and then di-

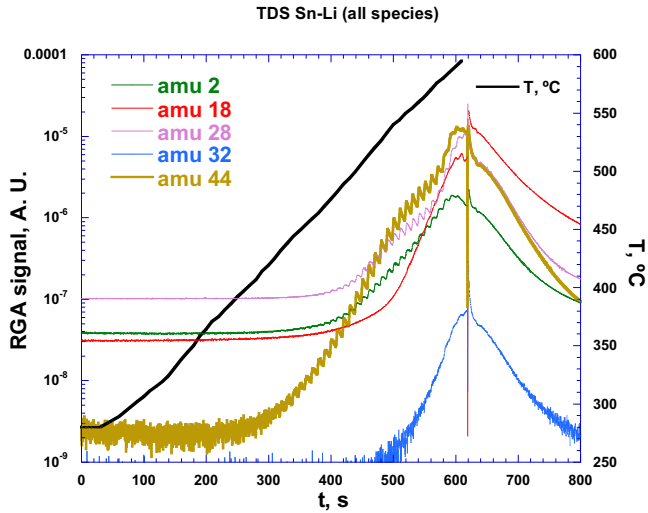


Fig. 8. TDS of the LiSn finger after exposure to 50 plasma shots. A significant contribution to mass 2 (H_2) can be ascribed to cracking of water in the ionization chamber of the QMS.

vided by the total amount of exposed $Li_{20}Sn_{80}$ (in all cases 0,12 mol). Fig. 2 shows the comparison of the results of H equilibrium mole fraction (X_H) of the present experiments and the results from previous literature data [4]. The results in the literature are for higher temperatures and higher exposure pressures than the present study but they show a linear relation between the square root of the equilibrium pressure and the equilibrium H mole fraction (Sieberts' law) for the two mixtures under study ($Li_{57}Sn_{43}$ and $Li_{62}Sn_{38}$). This linear relation can be used to compare with the present results.

As it can be observed, the results in the present work are in good agreement with the line fitted to the results obtained in the literature data. In our case there is some effect of the absorption temperature on the slope of the line, indicating lower H equilibrium concentration for lower temperatures while in the literature no remarkable changes with temperature are reported. It has to be taken into account that the temperature range in their experiments is higher (from 525 to 800 °C).

For the case of 1 Torr (133 Pa) exposure (the approximate pressure expected in a reactor divertor) the equilibrium H concentration is below 1.10^{-4} for the three temperatures studied. These values are more than two orders of magnitude smaller than for the case of pure lithium. Also, in the LiSn case, no hydride formation takes place at the relevant divertor pressures and temperatures, while for the case of pure lithium a certain temperature (above ~ 500 °C) would be needed in order to avoid the formation of LiH. It should also be noted that the resulting H uptakes here found are in good agreement with those obtained in hot plasma experiments for the same alloy [3] thus suggesting that no significant difference between plasma and gas exposure behaviour exists.

4.2. TJ-II exposure

The results obtained in TJ-II, partially displayed in Figs. 3–7, indicate good compatibility of the LiSn alloy held in a mesh structure (CPS arrangements) with hot stellarator plasmas. No significant increase of plasma contamination leading to enhanced radiation or fuel dilution has been seen. The observed behaviour fits well into the picture previously obtained from laboratory data. The strong enrichment of the surface of the alloy by lithium segregation makes it indistinguishable from pure lithium metal. However,

and contrary to what has been previously postulated [2], no melting of the alloy may be required in order to produce a Li rich surface according to our data. However, in situ surface analysis of the alloy “as prepared” would be required in order to determine whether Li surface segregation takes place due to the cooling method (inertial) used during its preparation or by plasma induced effects.

Although Li emission from the cold samples seems to be delayed by 50–80 ms respect to the hot finger case, as seen in Fig. 6, one would expect to see Sn emission by sputtering in the absence of surface segregation for solid LiSn samples. This is not the case, even when LCFS electronic temperatures in the range of 50 eV are commonly recorded by the He beam diagnostic and Langmuir probes. Moreover, local recycling was seen to be independent of the initial temperature (physical state) of the alloy, as displayed in Fig. 7. The fact that plasmas with higher densities achieve a higher, slowly increasing recycling value within the duration of the shot may indicate the achievement of the H equilibrium concentration on the sample during the discharge. For the typical edge parameters, with densities at the LCFS of $\sim 1 \times 10^{12} \text{ cm}^{-3}$, particle fluxes of $\sim 10^{18} \text{ cm}^{-2} \text{ s}^{-1}$ are to be expected. For an exposure area of 3 cm^2 , a concentration of 0.1% H/LiSn will be achieved in $< 2 \text{ s}$ while only 0.2 s (typical discharge duration) will be required for the values of 0.01% found in the laboratory tests. However, as the emission of $H\alpha$ from the finger was not systematically recorded from the beginning of the exposure to the plasma, the data presently available do not allow for a reliable assessment of this important parameter and more experiments will be required.

Although no direct recording of the surface sample temperature during the shots was made, the time evolution of the Li signals indicate that evaporation rather than erosion by the plasma (basically constant for the edge characteristics of the present discharges) dominate its intensity. Assuming a temperature dependence of Li evaporation from the alloy identical to that of pure Li (but with absolute values much smaller) a first estimate of the temperature excursions of the sample surface can be made.

The evaporation flux of a Li sample can be expressed as [9]:

$$\Gamma_{\text{vap}} = 1/4 n_{\text{Li}} \cdot V_{\text{Li}} = A \cdot P_{\text{vap}}(T) \cdot T^{-1/2} \quad (1)$$

where A is a proportionality factor and $P_{\text{vap}} = C \cdot 10^{(18.4 - 18,750/T)}$. For pure Li, if P_{vap} is expressed in Pa, $C = 133.3$, while for LiSn alloys, a factor of $\cong 1000$ reduction in P_{vap} has been previously reported [10].

For full ionization of Li into the edge plasmas, the photon flux, I_{Li} is proportional to the incoming flux from the sample. This flux will evolve in time as the temperature of the finger rises due to the plasma load. Assuming a semi-infinite slab model for the thermal response of the finger, one has:

$$\Delta T = 2Q \sqrt{t} / \sqrt{\pi k c_p \rho} \quad (2)$$

where Q is the thermal load (Wm^{-2}), k the thermal conductivity of the surface, c_p the specific heat of the alloy and ρ its density. By substituting T in Eq. (1) by the expected square root time dependence given by Eq. (2), then fitting the $\ln I_{\text{Li}}(t)$ vs. t curve, a value of the “thermal parameter” $2Q/\sqrt{\pi k c_p \rho}$ can be obtained. Example of this kind of fitting for two initial temperatures of the finger, 400 and 730 K, are shown in Fig. 9. As seen, a very good fitting to the expected behaviour is obtained by using a common value of the thermal parameter of $22 \text{ s}^{-1/2}$ for both cases. However, if the tabulated values of k, c_p and ρ for a LiSn mixture are assumed [10], values of Q up to 4 times higher than those deduced from the experimental edge parameters [11] are obtained. This would be in line with a strongly reduced thermal conductivity, k, of the damaged (corroded) SS CPS, visually observed after the experiments.

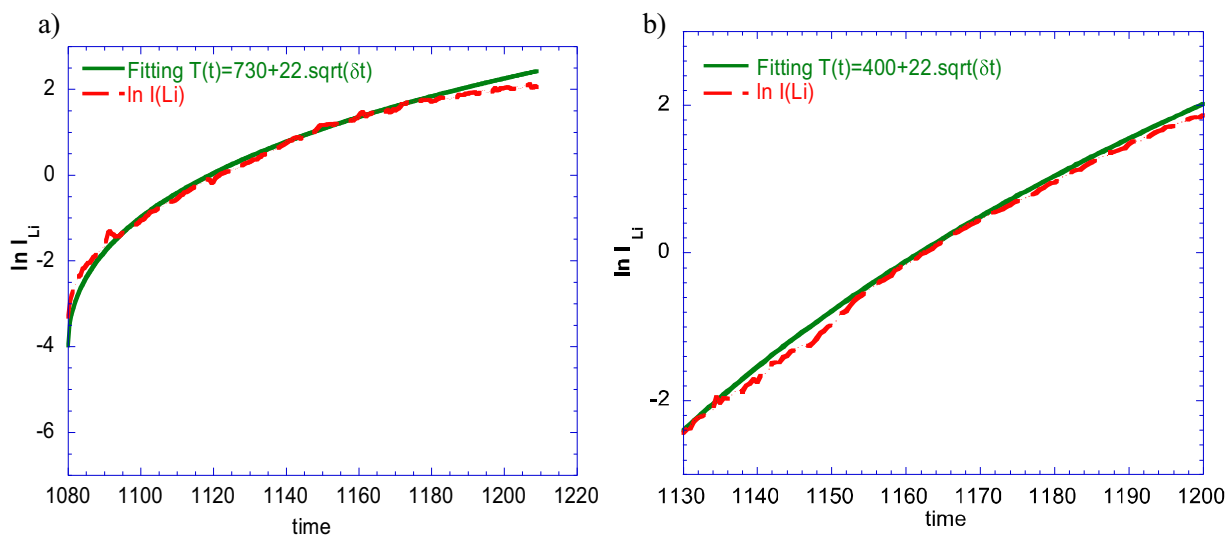


Fig. 9. Fitting of the lithium signal to the behaviour predicted by Eqs. (1) and (2). Left: initial temperature 730 K. Right: Initial temperature 400 K. Note the different time scales in both plots.

Direct temperature recordings by optical pyrometer and the use of W or Mo meshes are now foreseen to address this important issue.

5. Summary and conclusions

First tests of compatibility of a Li/Sn alloy with stellarator, hot plasmas have been performed in TJ-II. In addition, complementary laboratory experiments of H retention by the alloy were carried out at several temperatures and gas pressures.

The results obtained are summarized below:

- H retention values of $\sim 0.01\%$ H/(Sn+Li) at $T < 450^\circ\text{C}$ were deduced from TDS at the laboratory (gas exposure).
- Agreement with previous reports and in situ TDS in TJ-II.
- Insertion of a LiSn sample into the edge of TJ-II does not lead any significant perturbation of plasma parameters. Zeff values typically below 1.5 and very low Prad/Pin values ($< 2\%$) were deduced even with hot samples at the LCFS.
- Conversely, plasma operation became impossible if the SS support (finger) is uncovered.
- Only Li emission was detected. No traces of Sn were detected by visible and UV spectroscopy.
- H recycling did not evolve with temperature.
- Poor thermal conductivity of the CPS of LiSn was deduced for a damaged SS mesh.

These results provide good perspectives for use of LiSn alloys as a PFC in a Reactor.

Acknowledgements

This work has been carried out within the framework of the EUROfusion Consortium, WP PFC, and has received funding from the Euratom research and training program 2014–2018 under grant agreement No 633053. The views and opinions expressed herein do not necessarily reflect those of the European Commission.

References

- [1] M.A. Abdou, et al., On the exploration of innovative concepts for fusion chamber technology, *Fusion Eng. Des.* 54 (2001) 181–247.
- [2] J.P. Allain, et al., *J. Nucl. Mater.* 290–293 (2001) 33.
- [3] J. Loureiro et al. Proc ISLA-4 Conference. Granada. Sept 2015 (to appear in *Fusion Eng. Des.*). Also in this Conference.
- [4] C. John Wen, R.A. Huggins, Thermodynamic study of the lithium-tin system, *J. Electrochem Soc.* 128 (1981) 1181.
- [5] R. Schumacher, A. Weiss, H solubility in the liquid alloys lithium-indium, lithium-lead and lithium-tin, *Ver Bunsenges Phys. Chem.* 94 (1990) 648.
- [6] F.L. Tabarés, et al., Studies of plasma-lithium interactions in TJ-II, in: Proc. IAEA Conference, San Diego CA, 2012 P5/36.
- [7] F.L. Tabarés, et al., Effect of Li coating in plasma confinement and performance in TJ-II, *Plasma Phys. Control. Fusion* 50 (2008) 124051.
- [8] F.L. Tabarés, et al., Testing the compatibility of lithium elements with a hot plasma: studies of solid lithium insertion in TJ-II, Proc 39th EPS Conf. Stockholm, 2012.
- [9] A.F. Mills, *Heat Transfer*, second ed., Prentice Hall, Inc., Upper Saddle River, New Jersey, 1999.
- [10] S. Sharafat, N. Ghoniem, Summary of Thermo-Physical Properties of Sn and Compounds of Sn–H, Sn–O, Sn–C, Sn–Li, Sn–Si and Comparison of Properties of Sn, Sn–Li, Li, University of California, 2000 Pb–Li Technical Report UCLA-UCMEP-00-31.
- [11] F.L. Tabarés, et al., First liquid lithium limiter biasing experiments in the TJ-II stellarator, *J. Nucl. Mater.* 463 (2015) 1142.